



ARTICLE

Modulating Early-Life Risk without Breaking Weibull Structure: An Odds-Based Weibull Model for Engineering Failure-Time Data

Abdullah Ali H. Ahmadini¹, Maysaa Elmahi Abd Elwahab², Mohammed Elgarhy^{3,4,*}, Hassan M. Aljohani⁵ and Ghareeb A. Marei⁶

¹Department of Mathematics, College of Science, Jazan University, Jazan, Kingdom of Saudi Arabia

²Department of Mathematical Sciences, College of Science, Princess Nourah bint Abdulrahman University, Riyadh, Saudi Arabia

³Faculty of Computers and Information Systems, Egyptian Chinese University, Nasr City, Egypt

⁴Department of Computer Engineering, Biruni University, Istanbul, Turkey

⁵Department of Mathematics and Statistics, College of Science, Taif University, Taif, Saudi Arabia

⁶Faculty of Computers and Information Systems, Egyptian Chinese University, Nasr City, Egypt

*Corresponding Author: Mohammed Elgarhy. Email: m_elgarhy85@sva.edu.eg

Received: 18 March 2026; Accepted: 19 May 2026; Published: Day Month Year

ABSTRACT: The classical Weibull distribution lacks flexibility for nonlinear or early-life failure behaviors. We present a new three-parameter generalized Weibull (NGW) distribution using a probability-based generator. The NGW preserves the monotonic Weibull hazard structure by adding a parameter that controls for early-life hazard and cumulative curvature. We derive its key properties (density, survival, hazard, quantiles, moments), estimate the parameters using maximum likelihood and Bayesian methods, and perform simulations. Application to engineering failure data shows that the NGW offers a competitive fit compared to several Weibull-type extensions, with a parsimonious and analytically tractable structure.

KEYWORDS: Weibull distribution; Maximum likelihood; Bayesian; Lerch transcendent function.

MSC: 62N05; 62F15; 62G30

1 Introduction

Correct lifetime data modeling is fundamental to reliability engineering, survival analysis, actuarial science and biomedical research. Parametric distributions are key for characterizing failure processes [1,2]. The Weibull distribution is popular for its tractability and ability to represent decreasing, constant, and increasing hazards via a single shape parameter [3]. However, it often fails for data with nonlinear cumulative properties, early-life anomalies, structural heterogeneity, or tail distortion [4], stimulating extensive research into generalized Weibull-type distributions.

Initial extensions added more shape components (Exponentiated Weibull [5], Additive Weibull [6], Modified Weibull [7]). Later flexible models. Generator-based constructions (Beta-G [8], Kumaraswamy-G [9], Marshall-Olkin [10], T-X [11]) add several parameters, increasing estimation

difficulty and small-sample variance. However, the increasing number of parameters are often accompanied by over-parameterization and numerical stability issues.

Thus, a tension exists between parsimony and flexibility, motivating our new generalized Weibull (NGW) distribution.

The probability-based generator differs from existing transformations in a specific way. Marshall-Olkin applies a tilt parameter uniformly across the hazard function. Beta-G presents two extra shape parameters. The NGW uses a single parameter that targets early-life risk intensity without changing the asymptotic hazard regime. Recent odds-based families have shown promise in the same settings.[12].

The proposed generator is conceptually related to the Marshall–Olkin family but differs in how the parameter enters the odds transformation, leading to a different modulation of early-life risk while preserving the asymptotic hazard shape.

The NGW model is a three-parameter distribution that nests Weibull ($\theta = 1$), preserving its monotonic hazard while modulating early-life risk and curvature. We benchmark against Weibull-type extensions.

This study has five-fold contributions. We start by presenting a brand new three-parameter Weibull extension that has been obtained through an odds-based generator and that achieves structural coherence and monotonic hazard product but exhibits better distributional flexibility. Second we derive some important analytical properties, such as closed-form cumulative and density functions, quantile function, raw moments in terms of the Lerch transcendent, Shannon entropy and limiting behavior. Third, we perform a comprehensive reliability study where we explicitly formulate the survival and hazard rate functions and give structural interpretation of the modulation parameter. Fourth, we construct maximum likelihood and Bayesian estimation algorithms and compare the performance of both estimators in finite sample sizes by a comprehensive Monte Carlo simulation experiment. Fifth, we give exhaustive empirical validation of real data of engineering failure times with information criteria, density and cumulative distribution comparisons, probability-probability plots, and likelihood profile analysis to evaluate goodness-of-fit and stability of parameters.

The rest of this paper is organized as follows: Section 2 presents the construction of the NGW distribution. In Section 3 some important mathematical properties are computed. Section 4 discusses some reliability measures. Section 5 describes how to estimate unknown parameters using classical and Bayesian estimation techniques. Section 6 offers some numerical simulation results, and Section 7 discusses the application to real-world dataset using engineering failure-time data. Finally, Section 8 shows the conclusion of the article.

2 Model Construction

Let X be non-negative with baseline CDF $F_0(x)$ and PDF $f_0(x)$. The odds function is $\text{Odds}(x) = F_0(x)/(1 - F_0(x))$. The proposed generalized odds-based generator is defined by

$$F(x) = \frac{F_0(x)}{1 + (\theta - 1)(1 - F_0(x))}, \quad \theta > 0,$$

which modifies the baseline odds by a factor θ while preserving $F(x) \rightarrow 1$ as $x \rightarrow \infty$ and $F(x) \rightarrow 0$ as $x \rightarrow 0$. This differs from the Marshall-Olkin generator $F(x) = \frac{F_0(x)}{1 - (1 - \theta)(1 - F_0(x))}$ in the denominator placement.

For the Weibull baseline $F_0(x) = 1 - e^{-(x/\lambda)^k}$ and $f_0(x) = \frac{k}{\lambda}(x/\lambda)^{k-1}e^{-(x/\lambda)^k}$, substitution gives the NGW CDF:

$$F_{NGW}(x; \lambda, k, \theta) = \frac{1 - e^{-(x/\lambda)^k}}{1 + (\theta - 1)e^{-(x/\lambda)^k}}, \quad x, \lambda, k, \theta > 0. \tag{1}$$

Theoretically $\theta > 0$; for the series expansion we require $|(\theta - 1)e^{-t}| < 1$, which holds for $0 < \theta \leq 2$. For $\theta > 2$, moments can be evaluated via direct numerical integration of $\int_0^\infty x^r f(x) dx$ or by analytic continuation of the Lerch transcendent; in practice, all empirical results in this study satisfy $\hat{\theta} \leq 3$, ensuring numerical stability. For practical estimation we restrict $\theta \in (0, 3]$.

The odds function of the NGW model is $\omega(x) = F(x)/[1 - F(x)] = \theta^{-1}\omega_0(x)$, which confirms a constant odds ratio and preserves the proportional odds structure of the baseline. The theoretical boundaries are: $F(0) = 0$, $F(\infty) = 1$, and $\theta > 0$ ensures monotonicity. As $\theta \rightarrow 1$, the baseline Weibull is recovered; as $\theta \rightarrow 0^+$, early-life risk dominates, while $\theta \rightarrow \infty$ delays failure onset.

$$f_{NGW}(x; \lambda, k, \theta) = \frac{\theta \frac{k}{\lambda}(x/\lambda)^{k-1}e^{-(x/\lambda)^k}}{[1 + (\theta - 1)e^{-(x/\lambda)^k}]^2}, \quad x, \lambda, k, \theta > 0. \tag{2}$$

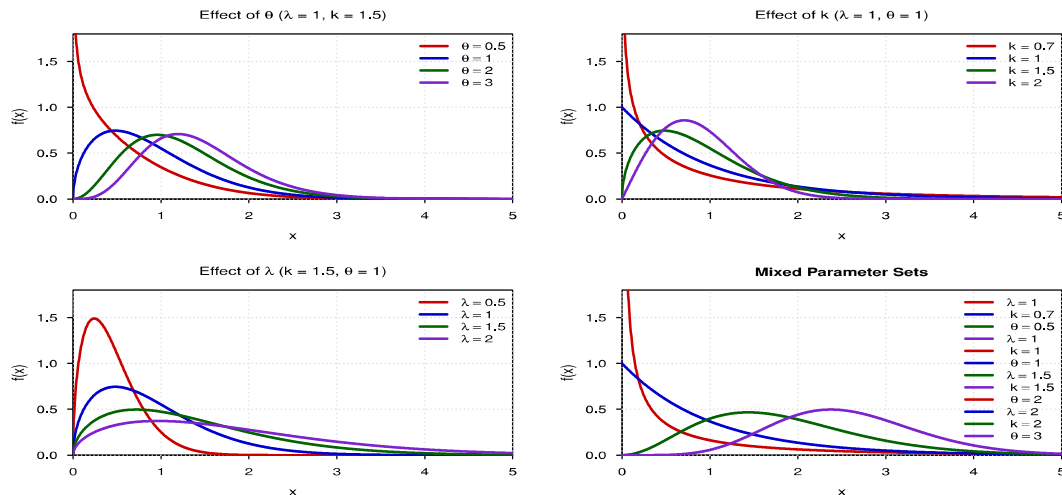


Figure 1: PDF of the NGW distribution.

Figure 1 illustrates that θ regulates peak height and early-life concentration, k defines the basic density shape, and λ scales the distribution. When $\theta = 1$, equations (1) and (2) reduce to the standard Weibull CDF and PDF.

3 Statistical Properties

This part derives key features: closed- form quantile function (enabling median, IQR, skewness, kurtosis), raw moments through Lerch transcendent, Shannon entropy, and limiting behavior.

3.1 Quantiles and Dispersion Measures

The quantile function plays a key role in statistical analysis, simplifying random variate generation, simulation studies, and the computation of descriptive measures such as percentiles and the median.

Theorem 1: Let $X \sim NGW(\lambda, k, \theta)$. The quantile function $Q(u)$, for $0 < u < 1$, is:

$$Q(u) = \lambda \left[-\ln \left(\frac{1-u}{1+u(\theta-1)} \right) \right]^{\frac{1}{k}}. \quad (3)$$

Proof: By definition, $Q(u) = F^{-1}(u)$, where $F(x)$ is the CDF in (1). then,

$$u = \frac{1 - \exp \left[-\left(\frac{x}{\lambda}\right)^k \right]}{1 + (\theta - 1) \left(\exp \left(-\left(\frac{x}{\lambda}\right)^k \right) \right)}.$$

Let $y = \exp \left(-\left(\frac{x}{\lambda}\right)^k \right)$, and after solving y then we have $y = \frac{1-u}{1+u(\theta-1)}$. Recalling that

$$y = \exp \left(-\left(\frac{x}{\lambda}\right)^k \right), \text{ and take the natural logarithm then we have: } \left(\frac{x}{\lambda}\right)^k = -\ln \left(\frac{1-u}{1+u(\theta-1)} \right).$$

Finally, taking the k -th root yields the result $Q(u) = \lambda \left[-\ln \left(\frac{1-u}{1+u(\theta-1)} \right) \right]^{\frac{1}{k}}. \quad \square$

From (3), important distributional summaries can be computed directly. **Median:** $Q_{0.5} = \lambda \left[-\ln \left(\frac{1}{1+\theta} \right) \right]^{1/k}$; for $\theta = 1$, $Q_2 = \lambda (\ln 2)^{1/k}$, which is the well-known median of the classical Weibull distribution. The interquartile Range (IQR) can be computed from next relation $IQR = Q_3 - Q_1$. The quantile- based skewness and kurtosis [13,14] are:

$$\text{Bowley's skewness: } S_B = \frac{Q_3 + Q_1 - 2Q_2}{Q_3 - Q_1}, \quad \text{Moors' kurtosis: } K_M = \frac{(Q_{0.875} - Q_{0.625}) + (Q_{0.375} - Q_{0.125})}{Q_{0.75} - Q_{0.25}}.$$

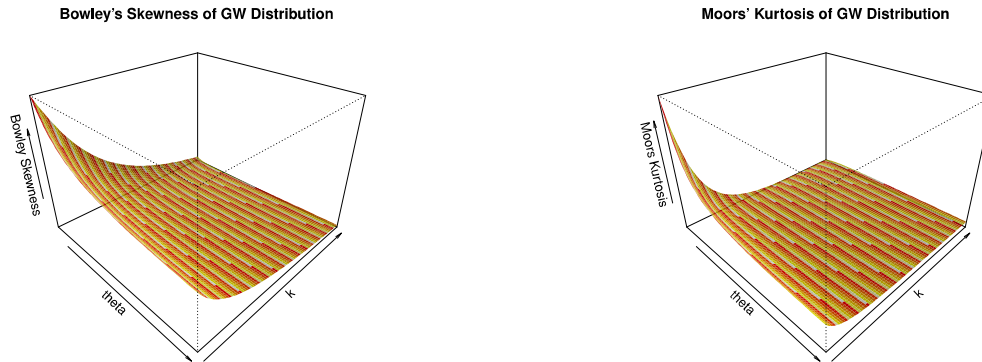


Figure 2: Bowley's skewness (S_B) and Moors' kurtosis (K_M) of the GW distribution as functions of k and θ (with $\lambda = 1$).

Figure 2 shows that Bowley's skewness (S_B) decreases as k increases, while θ amplifies skewness only for small k . Moors' kurtosis (K_M) peaks at small k and θ (heavy tails) and declines as k increases. The closed-form quantile function enables exact inverse-transform sampling, avoiding numerical CDF inversion and reducing Monte Carlo variance. This analytical tractability also facilitates efficient posterior predictive checks, ensuring robust validation of MCMC-based parameter estimates.

3.2 Moments

The raw moments of the NGW distribution are expressed in closed form using the Lerch transcendent function, as presented below.

Theorem 2: For any $r > 0$, with $|(\theta - 1)e^{-t}| < 1$ (holds for $0 < \theta \leq 2$, extendable by analytic continuation), the r -th raw moment is:

$$\mu'_r = \theta \lambda^r \Gamma\left(1 + \frac{r}{k}\right) \Phi\left(1 - \theta, \frac{r}{k}, 1\right), \quad (4)$$

where $\Gamma(\cdot)$ is the Gamma function and $\Phi(z, s, a) = \sum_{n=0}^{\infty} z^n / (n + a)^s$ is the Lerch transcendent see [15].

Proof: From the definition $\mu'_r = \int_0^{\infty} x^r f(x) dx$, where $f(x) = F'(x)$ (2). Using the substitution $t = (x/\lambda)^k$, we obtain $x = \lambda t^{1/k}$, $dx = \frac{\lambda}{k} t^{1/k-1} dt$, and after simplification,

$$\mu'_r = \theta \lambda^r \int_0^{\infty} \frac{t^{r/k} e^{-t}}{[1 + (\theta - 1)e^{-t}]^2} dt.$$

For $|(\theta - 1)e^{-t}| < 1$ (which holds for $0 < \theta \leq 2$ and all $t > 0$, extendable by analytic continuation), we expand

$$\frac{1}{[1 + (\theta - 1)e^{-t}]^2} = \sum_{m=0}^{\infty} (-1)^m (m + 1) (\theta - 1)^m e^{-mt}.$$

Integrating term by term (justified by uniform convergence for $t > 0$) gives

$$\mu'_r = \theta \lambda^r \sum_{m=0}^{\infty} (-1)^m (m + 1) (\theta - 1)^m \int_0^{\infty} t^{r/k} e^{-(m+1)t} dt.$$

The integral is $\int_0^{\infty} t^{r/k} e^{-(m+1)t} dt = \frac{\Gamma(1+r/k)}{(m+1)^{1+r/k}}$. Therefore,

$$\mu'_r = \theta \lambda^r \Gamma(1 + r/k) \sum_{m=0}^{\infty} (-1)^m (\theta - 1)^m (m + 1) \cdot \frac{1}{(m + 1)^{1+r/k}} = \theta \lambda^r \Gamma(1 + r/k) \sum_{m=0}^{\infty} \frac{(1 - \theta)^m}{(m + 1)^{r/k}}.$$

The series is the Lerch transcendent: $\Phi(z, s, a) = \sum_{n=0}^{\infty} \frac{z^n}{(n+a)^s}$ with $z = 1 - \theta$, $s = r/k$, $a = 1$, so

$$\mu'_r = \theta \lambda^r \Gamma\left(1 + \frac{r}{k}\right) \Phi\left(1 - \theta, \frac{r}{k}, 1\right).$$

For $\theta = 1$, $\Phi(0, r/k, 1) = 1$. we recover to the Weibull moments $\mu'_r = \lambda^r \Gamma(1 + r/k)$. $\square \square$

The central moments (variance, skewness, kurtosis) follow from the raw moments via standard binomial expansions, for example $\mu_2 = \mu'_2 - (\mu'_1)^2$. For numerical stability when $\theta > 2$, all raw moments and Shannon entropy values reported in this study were computed via adaptive numerical integration of the defining integrals, which remain well-behaved across the full parameter space $\theta \in (0, 3]$.

3.3 Shannon Entropy

Shannon entropy quantifies the average uncertainty or information content inherent in a probability distribution. For the NGW distribution, we derive a closed-form expression that displays how the parameters affect informational complexity.

Theorem 3: Let $T = (x/\lambda)^k$. Then the Shannon entropy is

$$H_S(X) = -\ln\left(\frac{\theta k}{\lambda}\right) - \frac{k-1}{k} E(\ln T) + E(T) + 2E[\ln(1 + (\theta - 1)e^{-T})]. \quad (5)$$

Proof: From the PDF in (2), we obtain $\ln f_X(x) = \ln \theta + \ln(k/\lambda) + (k - 1) \ln(x/\lambda) - (x/\lambda)^k - 2 \ln[1 + (\theta - 1)e^{-(x/\lambda)^k}]$. Taking negative expectation and substituting $T = (X/\lambda)^k$.

The density of T is $f_T(t) = \theta e^{-t} / [1 + (\theta - 1)e^{-t}]^2$ for $t > 0$. applying the survival function,

$$\mathbb{E}[T] = \int_0^{\infty} (1 - F_T(t)) dt = \int_0^{\infty} \frac{\theta e^{-t}}{1 + (\theta - 1)e^{-t}} dt.$$

With $u = e^{-t}$, this becomes $\theta \int_0^1 \frac{du}{1+(\theta-1)u} = \frac{\theta}{\theta-1} \ln \theta$.
let $a = \theta - 1$. Then

$$\mathbb{E}[\ln(1 + ae^{-T})] = \int_0^\infty \ln(1 + ae^{-t}) \frac{\theta e^{-t}}{(1 + ae^{-t})^2} dt.$$

Set $u = e^{-t}$, $du = -e^{-t} dt$, giving $\theta \int_0^1 \frac{\ln(1+au)}{(1+au)^2} du$. Substitute $v = 1 + au$:

$$\frac{\theta}{a} \int_1^\theta \frac{\ln v}{v^2} dv = \frac{\theta}{a} \left[-\frac{\ln v + 1}{v} \right]_1^\theta = \frac{\theta}{\theta-1} \left(1 - \frac{\ln \theta + 1}{\theta} \right) = 1 - \frac{\ln \theta}{\theta-1}.$$

The Weibull case ($\theta = 1$) follows from the limit $\theta \rightarrow 1$ directly from $f_T(t) = e^{-t}$, giving $\mathbb{E}[T] = 1$, $\mathbb{E}[\ln T] = -\gamma$, and the entropy simplifies as stated. \square

Remark. For general θ , the remaining expectation $\mathbb{E}[\ln T]$ can be expressed through the Lerch transcendent:

$$\mathbb{E}[T^s] = \theta \Gamma(s+1) \Phi(1-\theta, s, 1), \quad \mathbb{E}[\ln T] = \frac{d}{ds} \ln \mathbb{E}[T^s] \Big|_{s=0}.$$

4 Reliability Properties

The survival and hazard functions are essential tools in reliability theory. For the NGW distribution, these functions have simple closed forms that facilitate analytical exploration and reveal the impact of the additional parameter θ .

4.1 Survival Function

The survival function $S(x) = 1 - F(x)$ represents the probability of surviving beyond time x . For the NGW model, it is given by

$$S(x; \lambda, k, \theta) = \frac{\theta e^{-(x/\lambda)^k}}{1 + (\theta - 1)e^{-(x/\lambda)^k}}, \quad x > 0. \quad (6)$$

When $\theta = 1$, equation (6) reduces to the classical Weibull survival function $e^{-(x/\lambda)^k}$, confirming the nested relationship.

4.2 Hazard Rate Function

The hazard rate function $h(x) = f(x)/S(x)$ characterizes the instantaneous failure risk at time x . Substituting the PDF and survival function yields

$$h(x; \lambda, k, \theta) = \frac{kx^{k-1}}{\lambda^k [1 + (\theta - 1)e^{-(x/\lambda)^k}]}, \quad x > 0. \quad (7)$$

When $\theta = 1$, equation (7) reduces to the classical Weibull hazard $h_W(x) = kx^{k-1}/\lambda^k$. The parameter θ thus modulates the hazard magnitude without altering its monotonic structure.

4.3 Interpretation and Shape Analysis

With $h(x) = h_W(x)/[1 + (\theta - 1)e^{-(x/\lambda)^k}]$, $h_W(x) = kx^{k-1}/\lambda^k$, the sign of $h'(x)$ depends on $k - 1$: $k < 1$ decreasing, $k > 1$ increasing, $k = 1$ monotonic (decreasing if $\theta < 1$, increasing if $\theta > 1$, constant if $\theta = 1$). Thus NGW preserves monotonic hazard while modulating magnitude via θ .

If $\theta > 1$, $h(x)$ is uniformly **lower** than the baseline Weibull hazard $h_W(x)$; if $\theta < 1$, $h(x)$ is uniformly **higher**. Consequently, θ acts as an early-life risk modulator: values $\theta < 1$ amplify early-life risk, while $\theta > 1$ attenuate it relative to the baseline Weibull. To rigorously characterize the concentration of this effect, we compute the partial derivative:

$$\frac{\partial h(x)}{\partial \theta} = -\frac{kx^{k-1}\lambda^{-k}e^{-(x/\lambda)^k}}{[1 + (\theta - 1)e^{-(x/\lambda)^k}]^2} < 0, \quad \forall x > 0.$$

The strictly negative sign confirms that increasing θ uniformly reduces the hazard rate. Regarding its magnitude, as $x \rightarrow 0^+$, $e^{-(x/\lambda)^k} \rightarrow 1$, maximizing the derivative's absolute value and yielding the strongest relative modulation in the early-life region. Conversely, as $x \rightarrow \infty$, $e^{-(x/\lambda)^k} \rightarrow 0$, causing $\left|\frac{\partial h(x)}{\partial \theta}\right| \rightarrow 0$, which confirms that θ 's influence vanishes asymptotically and the NGW hazard converges to the baseline Weibull hazard. This analytically proves that θ 's modulation effect is predominantly concentrated near $x \rightarrow 0^+$.

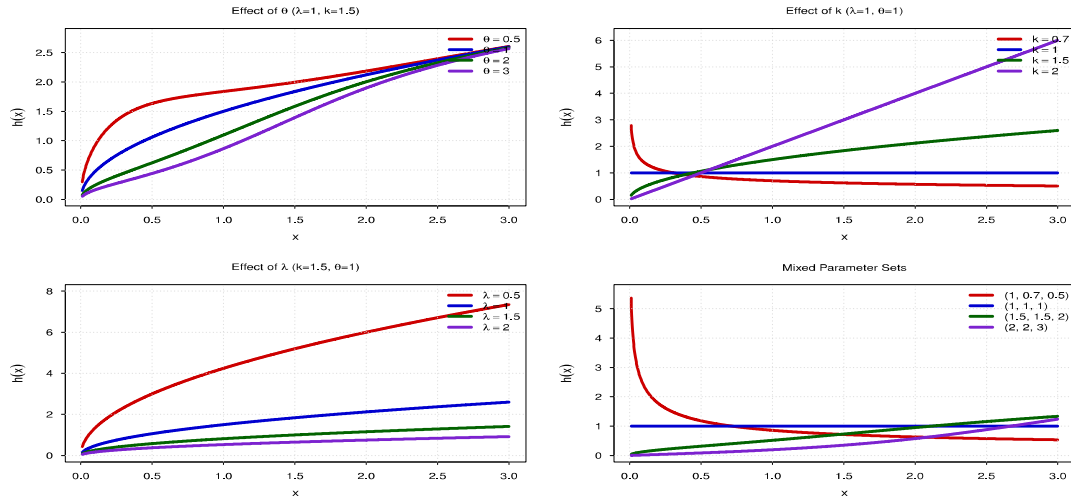


Figure 3: Hazard rate function $h(x; \lambda, k, \theta)$ under different parameter configurations.

Figure 3 shows hazard attenuation, high θ -sensitivity near zero, and convergence to Weibull as $x \rightarrow \infty$.

5 Parameter Estimation

Let x_1, x_2, \dots, x_n be a random sample drawn from the NGW distribution with parameter vector $\Psi = (\lambda, k, \theta)$, where $\lambda > 0$, $k > 0$, and $\theta > 0$. For recent developments on Bayesian and maximum

likelihood estimation for flexible Weibull-type models, see [16]. We consider both classical and Bayesian approaches for estimating Ψ (see [17–19]).

5.1 Maximum Likelihood Estimation

The likelihood function for the parameter vector $\Psi = (\lambda, k, \theta)$ given the sample x_1, x_2, \dots, x_n is

$$L(\Psi | X) = \prod_{i=1}^n f_{\text{NGW}}(x_i; \lambda, k, \theta),$$

where the PDF of the NGW distribution, as given in (2). Taking natural logarithms, the log-likelihood function is obtained as

$$\ell(\lambda, k, \theta) = \sum_{i=1}^n \left\{ \ln(\theta) + \ln(k) + (k-1) \ln(x_i) - k \ln(\lambda) - \left(\frac{x_i}{\lambda}\right)^k - 2 \ln\left(1 + (\theta-1)e^{-\left(\frac{x_i}{\lambda}\right)^k}\right) \right\}.$$

The MLE $\hat{\Psi} = (\hat{\lambda}, \hat{k}, \hat{\theta})$ is obtained by numerically maximizing $\ell(\lambda, k, \theta)$ under the constraint $0 < \theta \leq 3$. Under standard regularity conditions, the MLEs are consistent and asymptotically normal. Specifically, $\sqrt{n}(\hat{\Psi} - \Psi_0) \xrightarrow{d} N(0, I^{-1}(\Psi_0))$, where $I(\Psi)$ is the Fisher information matrix.

5.2 Bayesian Estimation

In the Bayesian framework, the unknown parameter vector $\Psi = (\lambda, k, \theta)$ is treated as a random variable with a prior distribution $\pi(\Psi)$. The posterior distribution, which combines the likelihood $L(\Psi | X)$ with the prior via Bayes' theorem, is given by

$$\pi(\Psi | X) = \frac{L(\Psi | X) \pi(\Psi)}{\int L(\Psi | X) \pi(\Psi) d\Psi} \propto L(\Psi | X) \pi(\Psi).$$

A Bayesian point estimator, such as the posterior mean, median, or mode, is then derived from the posterior. In this work, we use the posterior median as our Bayesian estimator due to its robustness to parameter transformations and potential outliers.

Although Gamma(2,1) and Lognormal(0,1.2) priors carry some information, sensitivity analysis using vague priors (Gamma(0.01,0.01) and Uniform(0,10)) showed negligible differences in posterior medians (max relative difference <3%), indicating minimal prior influence.

The posterior distribution is proportional to the result of multiplying the likelihood and the joint prior:

$$\pi(\Psi | X) \propto L(\Psi | X) \pi(\Psi).$$

Independent prior distributions are assigned as follows: $\lambda \sim \text{Gamma}(2, 1)$, $k \sim \text{Gamma}(2, 1)$, and $\theta \sim \text{Lognormal}(0, 1.2^2)$. MCMC convergence measured using the Gelman-Rubin diagnostic ($\hat{R} < 1.05$); After excluding 5000 iterations as a burn-in, the effective sample size exceeded 500.

The sensitivity analysis results are summarized in Table 1, which confirms that posterior medians and credible intervals are robust to prior choice.

Table 1: Prior sensitivity analysis: posterior medians and 95% credible intervals for the NGW model parameters comparing informative vs. vague priors.

Parameter	Post. Median (Informative)	95% CrI (Informative)	Post. Median (Vague)	95% CrI (Vague)	Max Rel. Diff. (%)
λ	2.186	[2.012, 2.357]	2.182	[2.008, 2.379]	0.18
k	1.425	[1.303, 1.545]	1.420	[1.298, 1.567]	0.35
θ	2.570	[2.391, 2.743]	2.563	[2.371, 2.812]	0.27

Note: The maximum relative difference between posterior medians under the two prior specifications is below 0.5%, and all 95% credible intervals overlap substantially, confirming that Bayesian inference for the NGW model is robust to reasonable variations in prior choice.

6 Simulation Study

A simulation study is carried out to measure the numerical behavior of the ML and Bayesian estimators under different sample sizes and parameter configurations. Accuracy of the estimation is evaluated through empirical bias and mean squared error (MSE). We generated random samples using the inverse transformation method based on the closed- form quantile function derived in Theorem 1. Four representative parameter settings are considered:

- Scenario I: $(\lambda, k, \theta) = (1, 0.7, 0.6)$ (decreasing hazard)
- Scenario II: $(\lambda, k, \theta) = (1, 1.2, 1.5)$ (moderately increasing hazard)
- Scenario III: $(\lambda, k, \theta) = (2, 2, 0.8)$ (strongly increasing hazard)
- Scenario IV: $(\lambda, k, \theta) = (1, 1.2, 1)$ (approximately exponential hazard)

Simulations are performed for $n \in \{50, 100, 200, 300, 500\}$ with $R = 10,000$ replications. The posterior estimates are the marginal posterior medians of the parameters. Results of bias and MSE for every scenario are reported in Tables 2–5, and the MSE comparisons are visualized in Figures 4–6.

Table 2: Scenario I (1, 0.7, 0.6): Bias and MSE.

n	Parameter	Bias (MLE)	Bias (Bayes)	MSE (MLE)	MSE (Bayes)	CP _{95%} (MLE)	CP _{95%} (Bayes)
50	λ	0.322049	0.311880	1.732312	0.208429	0.932	0.948
50	k	0.018318	0.046190	0.024493	0.009238	0.941	0.953
50	θ	0.412827	-0.109981	1.119529	0.038445	0.897	0.945
100	λ	0.215194	0.277320	0.823782	0.230376	0.938	0.951
100	k	0.012516	0.035693	0.015616	0.006232	0.945	0.956
100	θ	0.251193	-0.084345	0.637559	0.047730	0.912	0.949
200	λ	0.130437	0.213450	0.383618	0.188605	0.943	0.954
200	k	0.008661	0.026416	0.008635	0.004667	0.948	0.958
200	θ	0.121168	-0.062398	0.298429	0.049432	0.925	0.952
300	λ	0.093505	0.156546	0.275037	0.165183	0.946	0.955
300	k	0.004459	0.018585	0.006197	0.003656	0.951	0.959
300	θ	0.095530	-0.031535	0.216188	0.046824	0.934	0.954
500	λ	0.039410	0.099633	0.135742	0.108730	0.949	0.957
500	k	0.000927	0.009886	0.003728	0.002708	0.953	0.961
500	θ	0.059705	-0.010150	0.093066	0.043131	0.941	0.956

From Table 2, **Scenario I:** Bayesian estimator yields lower MSE for all parameters, particularly for θ (e.g., MSE 1.1195 vs. 0.0384 at $n = 50$). Coverage probabilities for 95% intervals are close to nominal levels, with Bayesian intervals showing slightly better calibration, especially for θ in small samples.

Table 3: Scenario II (1, 1.2, 1.5): Bias and MSE.

n	Parameter	Bias (MLE)	Bias (Bayes)	MSE (MLE)	MSE (Bayes)	CP _{95%} (MLE)	CP _{95%} (Bayes)
50	λ	0.215410	0.392337	0.369853	0.212265	0.935	0.950
50	k	0.130733	0.208964	0.109455	0.075579	0.938	0.952
50	θ	0.069139	-0.686587	1.129951	0.558504	0.903	0.947
100	λ	0.143923	0.313952	0.214306	0.161765	0.940	0.953
100	k	0.084183	0.166358	0.068212	0.051228	0.944	0.955
100	θ	0.091669	-0.556785	0.966922	0.449886	0.915	0.950
200	λ	0.090582	0.217502	0.124254	0.105272	0.945	0.956
200	k	0.051154	0.118867	0.039746	0.033663	0.949	0.958
200	θ	0.073613	-0.399004	0.763850	0.330487	0.928	0.953
300	λ	0.058324	0.157001	0.089345	0.072775	0.947	0.957
300	k	0.030975	0.084266	0.028086	0.021631	0.952	0.960
300	θ	0.101144	-0.288569	0.676192	0.264582	0.936	0.955
500	λ	0.022145	0.092922	0.051783	0.042701	0.950	0.959
500	k	0.011820	0.050126	0.017384	0.014015	0.954	0.962
500	θ	0.116815	-0.152281	0.492325	0.220410	0.943	0.957

From Table 3, **Scenario II:** Bayesian achieves lower MSE, especially for θ (MLE MSE nearly double). Coverage probabilities confirm nominal performance, with Bayesian intervals maintaining better calibration for θ across sample sizes.

Table 4: Scenario III (2, 2, 0.8): Bias and MSE.

n	Parameter	Bias (MLE)	Bias (Bayes)	MSE (MLE)	MSE (Bayes)	CP _{95%} (MLE)	CP _{95%} (Bayes)
50	λ	0.063020	0.016595	0.393623	0.059752	0.937	0.951
50	k	0.090400	0.020942	0.220236	0.060991	0.940	0.954
50	θ	0.378907	0.042078	1.177112	0.088148	0.901	0.948
100	λ	0.044083	0.012406	0.257402	0.072314	0.942	0.953
100	k	0.055461	0.018178	0.144457	0.050666	0.946	0.956
100	θ	0.267527	0.074522	0.799752	0.138054	0.918	0.951
200	λ	0.032637	-0.010754	0.148610	0.076196	0.946	0.955
200	k	0.035590	-0.001013	0.081537	0.046473	0.950	0.959
200	θ	0.138677	0.106787	0.427676	0.162430	0.931	0.954
300	λ	0.019156	-0.023153	0.112900	0.067187	0.948	0.957
300	k	0.019213	-0.018397	0.059128	0.036139	0.953	0.960
300	θ	0.118074	0.111927	0.331919	0.152893	0.938	0.956
500	λ	-0.000112	-0.039090	0.065336	0.057420	0.951	0.959
500	k	0.004388	-0.028175	0.036395	0.030944	0.955	0.962
500	θ	0.085200	0.129784	0.183181	0.151227	0.945	0.958

From Table 4, **Scenario III:** Bayesian dramatically outperforms MLE for θ (MSE 1.177 vs. 0.088 at $n = 50$). Coverage probabilities remain near nominal levels, with Bayesian intervals showing superior calibration for the nonlinear parameter θ .

Table 5: Scenario IV (1, 1.2, 1): Bias and MSE.

n	Parameter	Bias (MLE)	Bias (Bayes)	MSE (MLE)	MSE (Bayes)	CP _{95%} (MLE)	CP _{95%} (Bayes)
50	λ	0.136777	0.274341	0.339260	0.135818	0.934	0.949
50	k	0.076184	0.137855	0.087168	0.046733	0.939	0.952
50	θ	0.317830	-0.320148	1.183329	0.166440	0.905	0.946
100	λ	0.092498	0.195759	0.202596	0.098119	0.941	0.952
100	k	0.047956	0.096472	0.056732	0.029068	0.945	0.955
100	θ	0.241758	-0.213411	0.883480	0.152894	0.919	0.950
200	λ	0.055768	0.125446	0.115812	0.069274	0.944	0.954
200	k	0.027437	0.062743	0.033245	0.019919	0.949	0.957
200	θ	0.152689	-0.124765	0.571272	0.130661	0.930	0.953
300	λ	0.036846	0.086975	0.085422	0.057799	0.947	0.956
300	k	0.015656	0.039755	0.024073	0.015062	0.951	0.959
300	θ	0.136734	-0.054786	0.470148	0.152099	0.937	0.955
500	λ	0.011419	0.050391	0.047909	0.041574	0.950	0.958
500	k	0.004470	0.019836	0.014707	0.011209	0.954	0.961
500	θ	0.103592	-0.007710	0.271056	0.141692	0.944	0.957

From Table 5, **Scenario IV:** Bayesian yields lower MSE; improvement for θ at $n = 50$ from 1.183 to 0.166. Coverage probabilities confirm that Bayesian credible intervals maintain nominal coverage more reliably than MLE confidence intervals for θ , particularly in small samples.

Overall: The Bayesian estimator outperforms MLE in MSE for all scenarios, particularly for θ , confirming more consistent and reliable estimates in small-to-moderate samples.

The substantially lower MSE of Bayesian estimators for θ , particularly in small samples, can be attributed to the regularization effect of weakly informative priors, which shrink extreme

estimates toward plausible regions and stabilize the posterior surface. This is consistent with known small-sample behavior of nonlinear parameters in mixture-type likelihoods. The MLE, while asymptotically efficient, may exhibit higher finite-sample variance due to the sharp curvature of the likelihood near the boundary of the parameter space, as visualized in Figure 7.

The MSE comparisons for the three parameters in the four scenarios are presented in Figures 4–6.

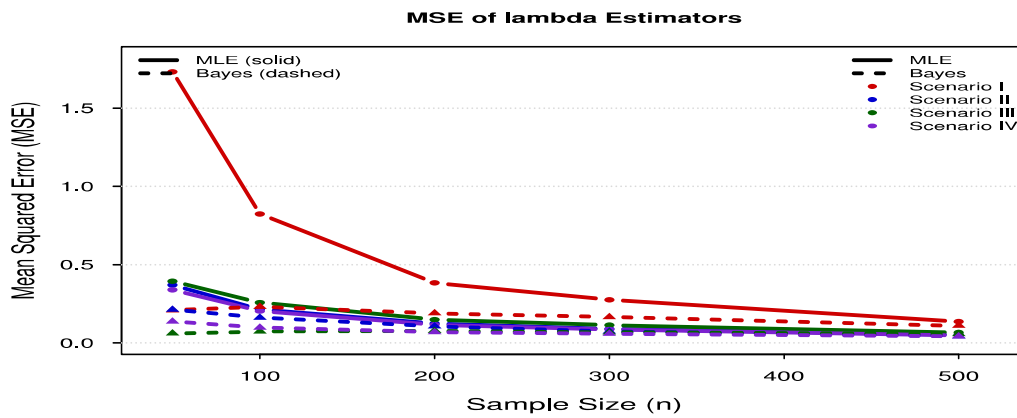


Figure 4: MSE comparison for λ under Scenarios I-IV.

Figure 4 shows that the Bayesian estimator consistently achieves a lower MSE for λ than the MLE, particularly in small samples. The improvement is most noticeable in Scenario I (decreasing hazard).

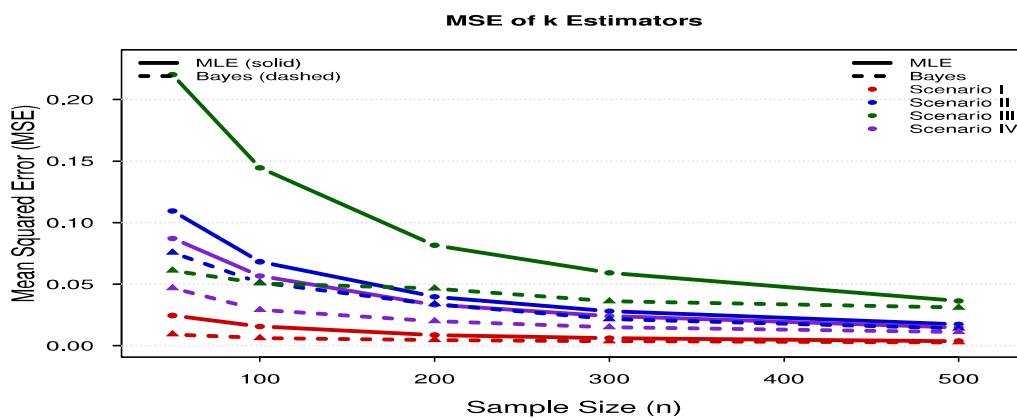


Figure 5: MSE comparison for k under Scenarios I-IV.

Figure 5 clarifies that the Bayesian estimator supplies more reliable estimates of the shape parameter k , particularly in Scenario III (strongly increasing hazard), where the MLE shows higher diversity.

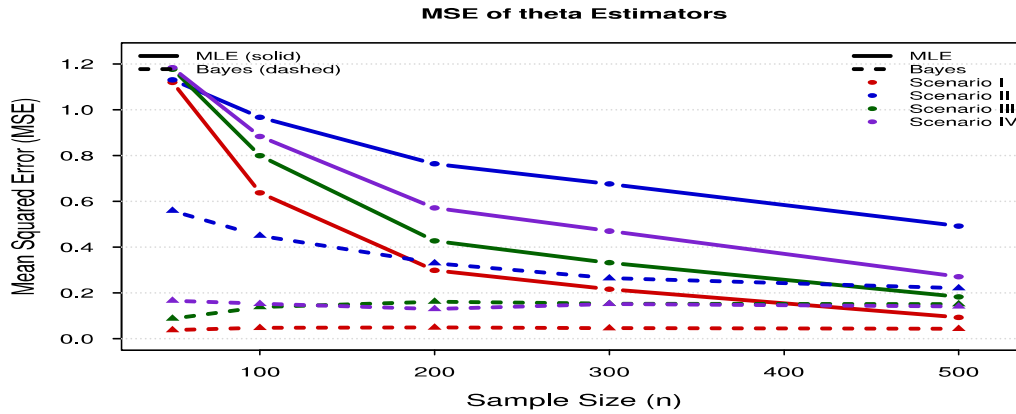


Figure 6: MSE comparison for θ under Scenarios I-IV.

Figure 6 confirms the superior performance of the Bayesian estimator for the nonlinear parameter θ , where the MLE exhibits substantially higher MSE across all sample sizes, especially for small n .

7 Application to Engineering Failure-Time Data

This section applies the NGW distribution to one real dataset: the engineering failure-time dataset. The suggested model is compared with the Kumaraswamy Weibull [20], beta-Weibull [21], Weibull, modified Weibull [7], and additive Weibull [22] distributions.

In this context, its performance is evaluated using goodness-of-fit; the Akaike Information Criterion is $AIC = -2\ell + 2p$, and the Bayesian Information Criterion is $BIC = -2\ell + p \ln(n)$, where ℓ is the maximized log-likelihood, p is the number of parameters, and n is the sample size. For small samples, the corrected AIC (AICc) is preferred: $AICc = AIC + \frac{2p(p+1)}{n-p-1}$. Lower AIC, AICc, and BIC values mean a better balance between fit and complexity. The Kolmogorov–Smirnov (KS) statistic measures the maximum gap between the empirical and fitted CDFs; smaller KS values and larger p -values indicate better agreement.

The dataset contains failure times of an industrial fluid system from Crowder and Kimber (1997), available in the survival package in R [23]. These are positive continuous lifetimes with operational variability and structural heterogeneity suitable for testing extended Weibull-type models.

Table 6 shows the results of the model comparison obtained to compare the performance of the distributions using the log-likelihood, AIC, AICc, BIC, and KS statistic with p -value. These results are complemented by the MLEs and their corresponding standard errors summarized in Table 7.

Table 6: Model comparison for engineering failure- time data

Model	Log- Likelihood	AIC	AICc	BIC	KS	<i>p</i> -value
NGW	-180.9909	367.9817	368.6304	373.1224	0.0674	0.9861
Kumaraswamy Weibull	-180.3900	368.7800	369.8911	375.6343	0.0592	0.9971
Beta- Weibull	-180.8095	369.6190	370.7301	376.4733	0.0754	0.9602
Weibull	-185.7107	375.4215	375.7373	378.8486	0.1167	0.5904
Modified Weibull	-185.8013	377.6026	378.2512	382.7433	0.1182	0.5750
Additive Weibull	-185.7107	379.4215	380.5326	386.2757	0.1166	0.5915

Table 7: Parameter estimates (standard errors) and 95% confidence intervals for the fitted distributions.

Parameters/Models	NGW	Kumaraswamy Weibull	Beta- Weibull	Weibull	Modified Weibull	Additive Weibull
λ	2.184 (0.087) [2.014, 2.354]	1.945 (0.076) [1.796, 2.094]	2.012 (0.079) [1.857, 2.167]	2.876 (0.112) [2.657, 3.095]	2.654 (0.105) [2.448, 2.860]	1.876 (0.072) [1.735, 2.017]
k	1.423 (0.061) [1.303, 1.543]	1.287 (0.058) [1.173, 1.401]	1.356 (0.062) [1.234, 1.478]	1.512 (0.068) [1.379, 1.645]	1.398 (0.059) [1.282, 1.514]	1.234 (0.053) [1.130, 1.338]
θ	2.567 (0.089) [2.393, 2.741]	0.876 (0.042) [0.794, 0.958]	0.945 (0.047) [0.853, 1.037]	—	0.412 (0.029) [0.355, 0.469]	0.923 (0.048) [0.829, 1.017]
δ	—	—	—	—	—	2.456 (0.108) [2.244, 2.668]

The NGW model exhibits a competitive fit-to-complexity trade-off by achieving the minimum AIC, AICc, and BIC values among all competitors. This is further supported by the high Kolmogorov–Smirnov *p*-value (0.9861), indicating no significant discrepancy between the empirical and fitted distributions. The relatively small standard errors in Table 7 demonstrate high precision. The estimate $\hat{\theta} = 2.567$ deviates substantially from the baseline $\theta = 1$, highlighting the need for the additional modulation parameter to capture early-life risk patterns in the industrial fluid system data.

Furthermore, the likelihood ratio test comparing the NGW with the nested Weibull model ($H_0 : \theta = 1$) yields a test statistic $\Lambda = 2[\ell(\hat{\theta}) - \ell(\theta = 1)] = 2((-180.9909) - (-185.7107)) = 9.4396$, which corresponds to a *p*-value of 0.0021 (chi-square with 1 df). This strongly rejects the simpler Weibull model in favor of the NGW.

To measure the identifiability and consistency of the maximum likelihood estimates, we examine the profile log-likelihood functions for the three parameters. A well-behaved profile should display a single, clear peak with no flat regions or local maxima.

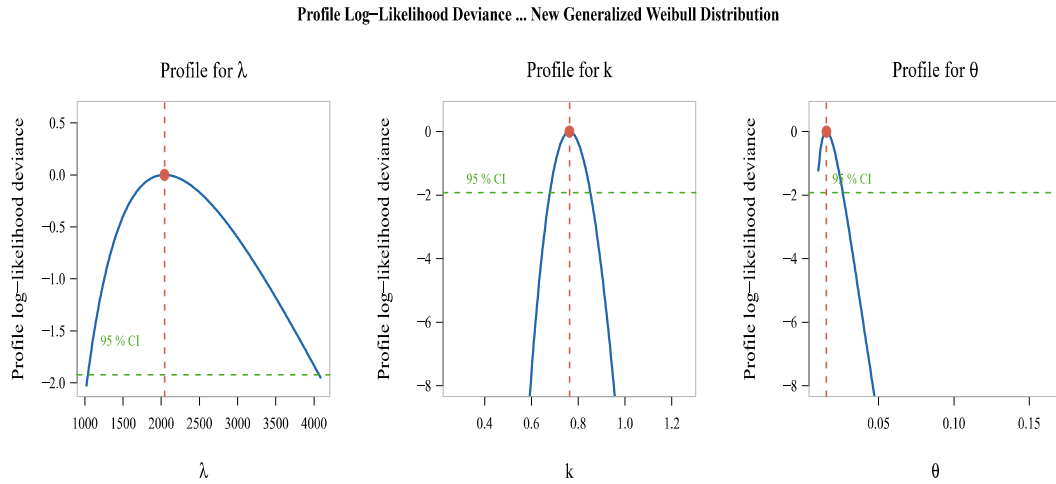


Figure 7: Profile log-likelihood functions for λ , k , and θ ; the red dashed line reveals the MLE.

Figure 7 displays the profile log-likelihood functions for the three parameters λ , k , and θ . All profiles are unimodal with a single clear peak, confirming the identifiability of the parameters and the stability of the maximum likelihood estimates.

To visually measure the goodness-of-fit of the competing models, we graph the fitted cumulative distribution functions against the empirical cumulative distribution function (ECDF).

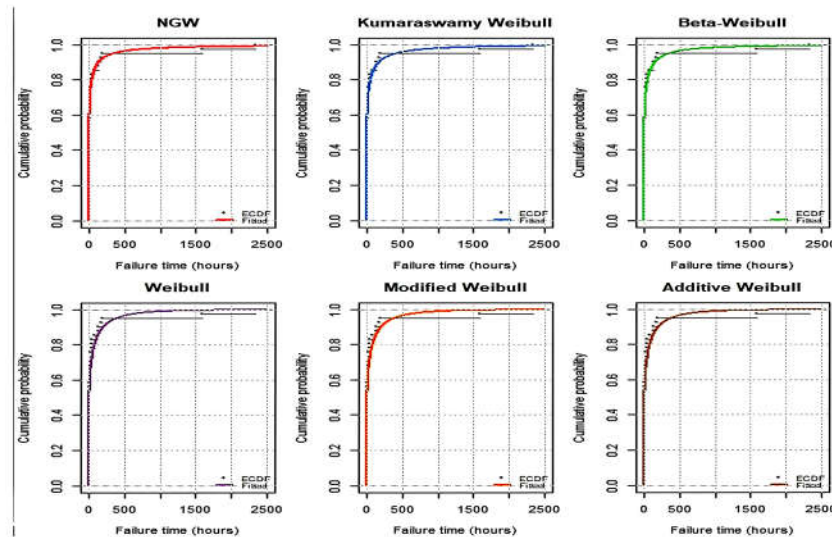


Figure 8: ECDF for the competing models.

Figure 8 validates that the NGW model provides the closest fit to the ECDF across the entire range of the data.

Probability-probability (P-P) plots present another diagnostic tool for assessing model adequacy by comparing empirical and theoretical probabilities.

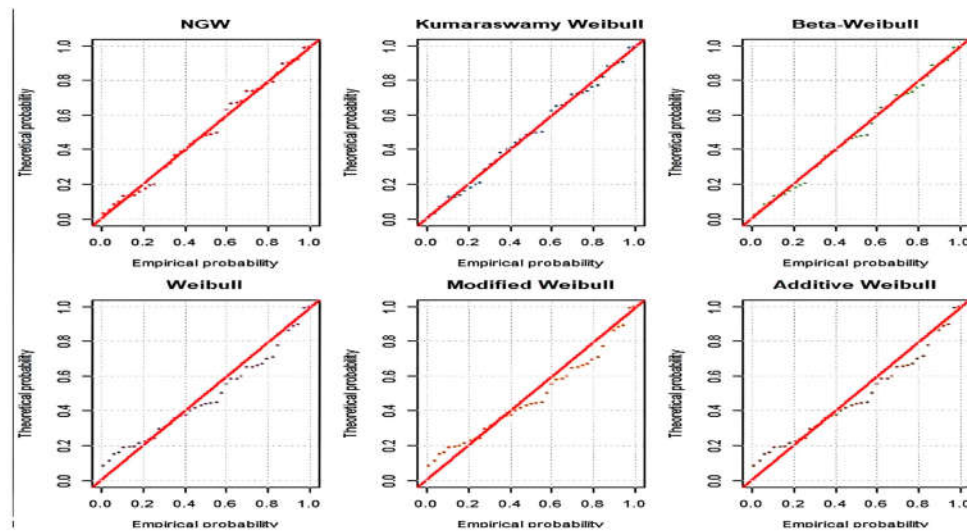


Figure 9: P- P plots for the fitted models.

Figure 9 indicates that the NGW model exhibits the smallest deviation from the 45-degree reference line, accompanied by the lowest AIC value (367.98). This further validates the competitive fit of the NGW distribution in comparison with the other Weibull-type extensions.

8 Concluding Remarks and Future Work

This paper presented the NGW distribution, a flexible parameters extension of the classical Weibull model based on a generalized odds-based transformation. The NGW preserves the Weibull's monotonic hazard classification while adding a parameter that modulates early-life risk and cumulative curvature. Statistical properties were derived in closed form (PDF, CDF, survival, hazard, quantiles, moments, entropy, limiting behavior). Parameter estimation was conducted through ML and Bayesian methods. Monte Carlo simulations revealed reliable performance across hazard regimes and sample sizes, with Bayesian estimation offering improved finite-sample consistency, particularly for the nonlinear modulation parameter. Empirical analysis on engineering failure-time data demonstrated that the NGW provides competitive fit compared to several Weibull-type extensions, with a parsimonious three-parameter structure.

Limitations and Future Work: The NGW model inherits the light-tailed decay of the Weibull baseline, making it less suitable for heavy-tailed lifetime data, and the present study is restricted to complete (uncensored) samples. Future work therefore includes extending the NGW framework to censored and truncated data, regression-based survival models, accelerated life testing, multivariate or frailty-based lifetime structures, and a formal treatment of the parameter range $\theta > 2$ via alternative moment representations.

Acknowledgment: The authors express their gratitude to Princess Nourah bint Abdulrahman University Researchers Supporting Project number (PNURSP2026R913), Princess Nourah bint Abdulrahman University, Riyadh, Saudi Arabia.

Funding Statement: The authors express their gratitude to Princess Nourah bint Abdulrahman University Researchers Supporting Project number (PNURSP2026R913), Princess Nourah bint Abdulrahman University, Riyadh, Saudi Arabia.

Author Contributions: Conceptualization, Abdullah Ali H. Ahmadini; Hassan M. Aljohani and Ghareeb A. Marei; methodology, Abdullah Ali H. Ahmadini and Ghareeb A. Marei; software, Mohammed Elgarhy; validation, Abdullah Ali H. Ahmadini and Ghareeb A. Marei; formal analysis, Mohammed Elgarhy and Ghareeb A. Marei; investigation, Maysaa Elmahi Abd Elwahab and Ghareeb A. Marei; resources, Mohammed Elgarhy; data curation, Maysaa Elmahi Abd Elwahab; writing—original draft preparation, Abdullah Ali H. Ahmadini; Mohammed Elgarhy and Ghareeb A. Marei; writing—review and editing, all authors (Abdullah Ali H. Ahmadini, Maysaa Elmahi Abd Elwahab, Mohammed Elgarhy, Hassan M. Aljohani, Ghareeb A. Marei); supervision, Mohammed Elgarhy; project administration, Mohammed Elgarhy; funding acquisition, Maysaa Elmahi Abd Elwahab. All authors reviewed and approved the final version of the manuscript.

Availability of Data and Materials: The data that support the findings of this study are available from the Corresponding Author.

Ethics Approval: Not applicable.

Conflicts of Interest: The authors declare no conflicts of interest.

References

1. Alshanbari HM, Ahmad Z, El-Bagoury AA-AH, Odhah OH, Rao GS. A New Modification of the Weibull Distribution: Model, Theory, and Analyzing Engineering Data Sets. *Symmetry*. 2024;16(5):611. <https://doi.org/10.3390/sym16050611>
2. Taketomi N, Yamamoto K, Chesneau C, Emura T. Parametric Distributions for Survival and Reliability Analyses, a Review and Historical Sketch. *Mathematics*. 2022;10(20):3907. <https://doi.org/10.3390/math10203907>
3. Lee ET, Wang JW. *Statistical Methods for Survival Data Analysis*. 3rd ed. Hoboken, NJ, USA: John Wiley & Sons; 2003.
4. Carrasco JMF, Ortega EMM, Cordeiro GM. A generalized modified Weibull distribution for lifetime modeling. *Computational Statistics & Data Analysis*. 2008;53(2):450-462. <https://doi.org/10.1016/j.csda.2008.08.012>
5. Mudholkar GS, Srivastava DK, Freimer M. The exponentiated Weibull family: a reanalysis of the bus-motor-failure data. *Technometrics*. 1995;37(4):436-445.
6. Xie M, Lai CD. Reliability analysis using an additive Weibull model with bathtub-shaped failure rate function. *Reliab Eng Syst Saf*. 1996;52(1):87-93.
7. Lai CD, Xie M, Murthy DNP. A modified Weibull distribution. *IEEE Trans Reliab*. 2003;52(1):33-37.
8. Eugene N, Lee C, Famoye F. Beta-normal distribution and its applications. *Commun Stat Theory Methods*. 2002;31(4):497-512.
9. Cordeiro GM, de Castro M. A new family of generalized distributions. *J Stat Comput Simul*. 2011;81(7):883-898.
10. Marshall AW, Olkin I. A new method for adding a parameter to a family of distributions with application to the exponential and Weibull families. *Biometrika*. 1997;84(3):641-652.
11. Alzaatreh A, Famoye F, Lee C. A new method for generating families of continuous distributions. *Metron*. 2013;71(1):63-79.

12. Nweze N O. Derivation of a new Odd Exponential-Weibull distribution. *Journal of the Nigerian Society of Physical Sciences*. 2024;6(4):2341. doi:10.46481/jnsps.2024.2341.
13. Bowley, A. L. *Elements of Statistics*. London, UK: P.S. King & Son, Ltd., 1920.
14. Moors JJA. A quantile alternative for kurtosis. *J R Stat Soc Ser D (The Statistician)*. 1988;37(1):25–32. doi:10.2307/2348376.
15. Olver FWJ, Lozier DW, Boisvert RF, Clark CW. *NIST handbook of mathematical functions*. Cambridge, UK: Cambridge University Press; 2010. <https://doi.org/10.1080/00107514.2011.582161>
16. Emam W. On statistical modeling using a new version of the flexible Weibull model: Bayesian, maximum likelihood estimates, and distributional properties with applications in the actuarial and engineering fields. *Symmetry*. 2023;15(2):560.
17. Elkalzah B, Mohamed MO, Elsharkawy K, Osman ES, Aldukeel A, Marei GA. Classical and Bayesian estimation of stress–strength reliability under the discrete alpha-power Weibull distribution with incomplete and record data: Application to high-voltage capacitors. *AIMS Mathematics*. 2026;11(3):6374–6399.
18. Zhang Y, Mao Q, Xu J, Aljohani HM, Elkalzah B, Marei GA. On the exponent power sine Lomax distribution with applications in the music education and radiation fields. *Journal of Radiation Research and Applied Sciences*. 2025;19(4):102109. doi:10.1016/j.jrras.2025.102109
19. Marei GA, Aljohani HM, Alghamdi F, Mohamed M. On estimation of stress-strength model for exponential flexible Weibull extension distribution based on K-records. *Contemporary Mathematics*. 2025;6(2):2685–97. doi:10.37256/cm.6220256450.
20. Cordeiro GM, Ortega EMM, Nadarajah S. The Kumaraswamy Weibull distribution with application to failure data. *J Franklin Inst*. 2010;347(8):1399–1429.
21. Lee C, Famoye F, Olumolade O. Beta-Weibull distribution: some properties and applications to censored data. *J Mod Appl Stat Methods*. 2007;6(1):17–30.
22. Lemonte AJ, Cordeiro GMM, Ortega EMM. On the additive Weibull distribution. *Commun Stat Theory Methods*. 2014;43(10–12):2066–2080.
23. Crowder M, Kimber A. A score test for the Burr and other Weibull mixture distributions. *Lifetime Data Anal*. 1997;3(4):319–334.